

Influence of the Electronics of the Phosphine Ligands on the H–H Bond Elongation in Dihydrogen Complexes

Saikat Dutta, Balaji R. Jagirdar,* and Munirathinam Nethaji

Department of Inorganic & Physical Chemistry, Indian Institute of Science, Bangalore 560 012, India

Received August 26, 2007

Five new monocationic dihydrogen complexes of ruthenium of the type $trans\text{-}[\text{RuCl}(\eta^2\text{-H}_2)(\text{PP})_2][\text{BF}_4]$ (PP = bis-1,2(diarylphosphino)ethane, aryl = *p*-fluorobenzyl, **1a**, benzyl, **2a**, *m*-methylbenzyl, **3a**, *p*-methylbenzyl, **4a**, *p*-isopropylbenzyl, **5a**) have been prepared by protonating the precursor hydride complexes $trans\text{-}[\text{RuCl}(\text{H})(\text{PP})_2]$ using $\text{HBF}_4\cdot\text{OEt}_2$. The dihydrogen complexes are quite stable and have been isolated in the solid state. The intact nature of the H–H bond in these derivatives has been established from the short spin–lattice relaxation times (T_1 , ms) and observation of substantial H, D couplings in the HD isotopomers. The H–H bond distances (d_{HH} , Å) increase systematically from 0.97 to 1.03 Å as the electron-donor ability of the substituent on the diphosphine ligand increases from the *p*-fluorobenzyl to the *p*-isopropylbenzyl moiety. The d_{HH} in $trans\text{-}[\text{Ru}(\eta^2\text{-H}_2)(\text{Cl})((\text{C}_6\text{H}_5\text{-CH}_2)_2\text{PCH}_2\text{CH}_2\text{P}(\text{CH}_2\text{C}_6\text{H}_5)_2)_2][\text{BF}_4]$, **2a**, was found to be 1.08(5) Å by X-ray crystallography. In addition, two new 16-electron dicationic dihydrogen complexes of the type $[\text{Ru}(\eta^2\text{-H}_2)(\text{PP})_2][\text{OTf}]_2$ (PP = $(\text{ArCH}_2)_2\text{PCH}_2\text{CH}_2\text{P}(\text{CH}_2\text{-Ar})_2$, Ar = *m*- $\text{CH}_3\text{C}_6\text{H}_4$ –, **6a**, *p*- $\text{CH}_3\text{C}_6\text{H}_4$ –, **7a**) have also been prepared and characterized. These derivatives were found to possess *elongated* dihydrogen ligands.

Introduction

The binding of molecular hydrogen to a metal center leads to elongation of the H–H bond and subsequently to its cleavage along the reaction coordinate for the oxidative addition of H_2 . There has been considerable interest in the study of the activation of dihydrogen and mapping out the reaction coordinate for the homolytic cleavage of H_2 on a metal center. A large number of dihydrogen complexes reported to date possess H–H distances ranging from 0.8 to 1.0 Å. Relatively fewer examples of *elongated* dihydrogen complexes are known, wherein the H–H distances fall in the range of 1.0–1.5 Å.^{1,2} In this regard, the study of the molecules that possess *elongated* dihydrogen moieties is of great interest because of the relevance and significance in important catalytic processes such as hydrogenation, hydrogenolysis, and hydroformylation. One of the current goals in this area is to study the smooth gradation of the H–H distances along the continuum

for the oxidative addition of H_2 to a metal center and find out at what point the H–H bond can be considered to be *broken*.

In order to realize complexes with H–H distances in this continuum, a very systematic study should be carried out by subtly varying the electron-donor abilities of the coligands in the complex such that the back-donation from the $\text{M}(\text{d}\pi)$ to the $\text{H}_2(\sigma^*)$ is increased in a systematic manner. For example, employing coligands that can be fine tuned by way of varying the substituents in a manner which will result in increased back-donation can lead to dihydrogen complexes with elongated H_2 ligands along the reaction coordinate for the oxidative addition of H_2 to a metal center. This can be achieved by employing phosphorus-based coligands since their steric as well as electronic properties can be varied in a very systematic manner. Kubas and co-workers studied the influence of the electronics of the substituted and unsubstituted benzyl diphosphine ligands on the dihydrogen versus dihydride coordination of a series of molybdenum complexes of the type $[\text{Mo}(\text{H}_2)(\text{CO})\{(\text{RCH}_2)_2\text{PCH}_2\text{CH}_2\text{P}(\text{CH}_2\text{R})_2\}]_2$. They found that the binding mode ($\eta^2\text{-H}_2$ or dihydride) is dictated by the nature of R: an $\eta^2\text{-H}_2$ complex is formed when R is an electron-withdrawing group, whereas a

* To whom correspondence should be addressed. E-mail: jagirdar@ipc.iisc.ernet.in.

(1) Kubas, G. J. *Metal Dihydrogen and σ Bond Complexes*; Kluwer Academic/Plenum Publishers: New York, 2001.

(2) Heinekey, D. M.; Lledós, A.; Lluch, J. M. *Chem. Soc. Rev.* **2004**, *33*, 175–182.

dihydride results when R is an electron-donating group.³ We earlier reported the influence of the sterics and electronics of certain phosphorus-containing ligands (trans to H₂ ligand) on the properties of the bound dihydrogen.⁴ In this paper, we report the synthesis and characterization of some new dihydrogen complexes of ruthenium bearing the bis(1,2-diarylphosphino)ethane ligands wherein the aryl group is a benzyl moiety with a substituent (*p*-fluoro, H, *m*-methyl, *p*-methyl, *p*-isopropyl). The electron-donor ability of the chelating phosphine in this series of complexes can be varied in a systematic manner by varying the substituent on the benzyl group. In combination with a good π donor like a chloride trans to the bound H₂ and by use of a suitable substituent, the donor ability of the chelating phosphine was increased in small increments along the series resulting in elongation of the H–H bonds in a systematic manner. In addition, we also report the synthesis and characterization of two new dicationic, 16-electron dihydrogen complexes in which the H–H bonds are elongated. Preliminary aspects of this work were communicated earlier.⁵

Experimental Section

General Procedures. All reactions were carried out under an atmosphere of nitrogen or argon at room temperature using standard Schlenk and inert atmosphere techniques unless otherwise noted.⁶ Solvents used for preparation of the dihydrogen complexes were thoroughly saturated with H₂ or Ar just before use. ¹H and ³¹P NMR spectral data were acquired using an Avance Bruker 400 MHz spectrometer. The ³¹P NMR spectra were recorded relative to 85% H₃PO₄ (aqueous solution) as an external standard. Variable-temperature ¹H T₁ measurements were carried out at 400 MHz using the inversion recovery method (180°– τ –90°).⁷ Mass spectral analyses were carried out using a Micromass Q-TOF instrument at the Department of Organic Chemistry, Indian Institute of Science. Magnesium required for the synthesis of the Grignard reagents was activated by the literature method.⁸ The ligands (ArCH₂)₂PCH₂CH₂P(CH₂Ar)₂ (Ar = *p*-FC₆H₄, C₆H₅–, *m*-CH₃C₆H₄–, *p*-CH₃C₆H₄–, *p*-^{*i*}PrC₆H₄–, *p*-^{*i*}BuC₆H₄–) and the metal complex [Ru(H)(Cl)(PPh₃)₃] were prepared adopting literature procedures.^{3,9} We reported the synthesis and characterization of *trans*-[Ru(H)(Cl)((C₆H₅CH₂)₂PCH₂CH₂P(CH₂C₆H₅)₂)₂], **2**, recently.⁵ (*p*-^{*i*}PrC₆H₄–CH₂)₂PCH₂CH₂P(CH₂–C₆H₄–*p*-^{*i*}Pr)₂ and (*p*-^{*i*}BuC₆H₄–CH₂)₂PCH₂CH₂P(CH₂–C₆H₄–*p*-^{*i*}Bu)₂ have not been reported previously.

Characterization Data for (*p*-^{*i*}PrC₆H₄–CH₂)₂PCH₂CH₂P(CH₂–C₆H₄–*p*-^{*i*}Pr)₂. ¹H NMR (CD₂Cl₂): δ 1.21 (d, 24H, ((CH₃)₂–

Table 1. ¹H and ³¹P{¹H} NMR Spectral Data (δ) of *trans*-[Ru(H)(Cl)((ArCH₂)₂PCH₂CH₂P(CH₂Ar)₂)₂] (Ar = *p*-FC₆H₄– (**1**), *m*-CH₃C₆H₄– (**3**), *p*-CH₃C₆H₄– (**4**), *p*-^{*i*}PrC₆H₄– (**5**)) Complexes in CD₂Cl₂

compd no./Ar	δ (Ru–H)	J (H,P _{cis}), Hz	H		J (H,H), Hz	δ (Ar–R)	δ (Ar)	³¹ P{ ¹ H}
			δ (CH ₂ CH ₂)	δ (CH ₂ Ar)				
1 / <i>p</i> -FC ₆ H ₄ – ^a	–19.86 (qnt, 1H)	19.7	0.92 (br s, 4H), 0.46 (br s, 4H)	2.81 (d, 4H), 3.00 (d, 4H), 3.18 (d, 4H), 4.22 (d, 4H)	15.1, 14.7, 14.7, 13.7	6.81–7.23 (br m, 32H)	63.2 (s)	
3 / <i>m</i> -CH ₃ C ₆ H ₄ –	–19.89 (qnt, 1H)	19.5	0.44 (br s, 4H), 0.89 (br s, 4H)	2.87 (d, 4H), 3.03 (d, 4H), 3.23 (d, 4H), 4.25 (d, 4H)	14.7, 13.7, 12.7, 13.7	6.75–7.41 (br m, 32H)	62.3 (s)	
4 / <i>p</i> -CH ₃ C ₆ H ₄ –	–19.92 (qnt, 1H)	19.7	0.41 (br s, 4H), 0.87 (br s, 4H)	2.78 (d, 4H), 3.00 (d, 4H), 3.11 (d, 4H), 4.16 (d, 4H)	14.6, 14.7, 14.7, 12.7	6.80–7.33 (br m, 32H)	63.9 (s)	
5 / <i>p</i> - ^{<i>i</i>} PrC ₆ H ₄ –	–19.98 (qnt, 1H)	20.0	0.48 (br s, 4H), 0.94 (br s, 4H)	2.31 (d, 4H), 3.43 (d, 4H), 4.19 (d, 4H) ^b	17.6, 14.6, 13.2	6.68–7.43 (br m, 32H), 2.86 (m, CH, 8H)	61.6 (s)	

^a ¹⁹F NMR: –116.5 (s), –117.6 (s). ^b The fourth doublet signal overlaps with the multiplet of the CH moiety of the ^{*i*}Pr group.

(3) Luo, X.-L.; Kubas, G. J.; Burns, C. J.; Eckert, J. *Inorg. Chem.* **1994**, *33*, 5219–5229.

(4) (a) Mathew, N.; Jagirdar, B. R.; Gopalan, R. S.; Kulkarni, G. U. *Organometallics* **2000**, *19*, 4506–4517. (b) Mathew, N.; Jagirdar, B. R.; Ranganathan, A. *Inorg. Chem.* **2003**, *42*, 187–197. (c) Nanishankar, H. V.; Nethaji, M.; Jagirdar, B. R. *Eur. J. Inorg. Chem.* **2004**, 3048–3056.

(5) Dutta, S.; Jagirdar, B. R. *Inorg. Chem.* **2006**, *45*, 7047–7049.

(6) (a) Shriver, D. F.; Drezdon, M. A. *The Manipulation of Air Sensitive Compounds*, 2nd ed.; Wiley: New York, 1986. (b) Herzog, S.; Dehnert, J.; Lühder, K. In *Technique of Inorganic Chemistry*; Johnassen, H. B., Ed.; Interscience: New York, 1969; Vol. VII.

(7) Hamilton, D. G.; Crabtree, R. H. *J. Am. Chem. Soc.* **1988**, *110*, 4126–4133.

(8) Karen, V.; Barker, J. M.; Brown, N. H.; Skarnulis, A. J.; Sexton, A. *J. Org. Chem.* **1991**, *56*, 698–703.

(9) (a) Schunn, R. A.; Wonchoba, E. R. *Inorg. Synth.* **1971**, *13*, 131–134. (b) Hallman, P. S.; McGarvey, B. R.; Wilkinson, G. *J. Chem. Soc. (A)* **1968**, *12*, 3143–3150.

CH)), 1.27 (br s, 4H, $-CH_2CH_2-$), 2.62 (d, 4H, CH_2Ar , $J(H,H) = 12.7$ Hz), 2.70 (d, 4H, CH_2Ar , $J(H,H) = 12.7$ Hz), 2.85 (sep, 4H, $(CH_3)_2CH$), $J(H,H) = 6.8$ Hz), 7.10 (d, 8H, C_6H_4 , $J(H,H) = 7.6$ Hz), 7.23 (d, 8H, C_6H_4 , $J(H,H) = 7.6$ Hz). $^31P\{^1H\}$ NMR (CD_2Cl_2): $\delta -14.6$ (s). QTOF-MS: $m/z = 621$ [M^+].

Characterization Data for $(p\text{-Bu}C_6H_4-CH_2)_2PCH_2CH_2P(CH_2-C_6H_4-p\text{-Bu})_2$. 1H NMR (C_6D_6): δ 1.20 (br s, 4H, $-CH_2CH_2-$), 1.29 (s, 36H, $(CH_3)_3C$), 2.65 (d, 4H, CH_2Ar , $J(H,H) = 13.8$ Hz.), 2.75 (d, 4H, CH_2Ar , $J(H,H) = 13.7$ Hz.), 6.99 (d, 8H, C_6H_4 , $J(H,H) = 7.8$ Hz), 7.09 (d, 8H, C_6H_4 , $J(H,H) = 7.8$ Hz). $^31P\{^1H\}$ NMR (C_6D_6): $\delta -14.7$ (s). QTOF-MS: $m/z = 678$ [M^+].

Preparation of $trans\text{-}[Ru(H)(Cl)(PP)_2]$ ($PP = (ArCH_2)_2PCH_2CH_2P(CH_2Ar)_2$, $Ar = p\text{-FC}_6H_4$, **1, C_6H_5 -, **2**, $m\text{-Me}C_6H_4$ -, **3**, $p\text{-Me}C_6H_4$ -, **4**, $p\text{-}^iPrC_6H_4$ -, **5**).** A mixture of $[Ru(H)(Cl)(PPh_3)_3]$ (0.100 g, 0.108 mmol) and $(p\text{-FC}_6H_4CH_2)_2PC_2H_4P(CH_2C_6H_4p\text{-F})_2$ (0.250 g, 0.475 mmol, ~ 2.5 equiv) in toluene (10 mL) was refluxed for 10 min. The purple solution turned yellow during this process. The reaction mixture was cooled to room temperature, and the volatiles were removed under vacuum. The yellowish-white solid product was washed using petroleum ether (3×5 mL) and then dried under vacuum to obtain a yellowish-white solid of $trans\text{-}[Ru(H)(Cl)((p\text{-FC}_6H_4CH_2)_2PC_2H_4P(CH_2C_6H_4p\text{-F})_2)_2]$, **1**. Yield: 0.065 g (50%). Compounds **2–5** were similarly prepared. The synthetic details for complexes **2–5** are given in the Supporting Information. The NMR spectral data of these complexes have been collected in Table 1. The mass spectral data of the complexes are as follows. **1**: $m/z = 1154$ [$M^+ - HCl$]. **2**: $m/z = 1011$ [$M^+ - Cl^-$]. **3**: $m/z = 1121$ [$M^+ - (H_2 + Cl^-)$]. **4**: $m/z = 1157$ [$M^+ - H^+$], 1122 [$M^+ - HCl$]. **5**: $m/z = 1346$ [$M^+ - HCl$].

Preparation of $trans\text{-}[Ru(\eta^2\text{-H}_2)(Cl)(PP)_2][BF_4]$ ($PP = (ArCH_2)_2PCH_2CH_2P(CH_2Ar)_2$, $Ar = p\text{-FC}_6H_4$ -, **1a, C_6H_5 -, **2a**, $m\text{-CH}_3C_6H_4$ -, **3a**, $p\text{-CH}_3C_6H_4$ -, **4a**, $p\text{-}^iPrC_6H_4$ -, **5a**).** A H_2 -saturated CH_2Cl_2 solution (10 mL) of $trans\text{-}[Ru(H)(Cl)((p\text{-FC}_6H_4CH_2)_2PC_2H_4P(CH_2C_6H_4p\text{-F})_2)_2]$, **1** (0.050 g, 0.042 mmol), was cooled to 273 K. To this solution, 54% $HBF_4 \cdot OEt_2$ (5.7 μ L, 0.043 mmol, 1 equiv) was added, and the reaction mixture was stirred for 10 min. Solvent was stripped under vacuum, and the solid residue of $trans\text{-}[Ru(\eta^2\text{-H}_2)(Cl)((p\text{-FC}_6H_4CH_2)_2PC_2H_4P(CH_2C_6H_4p\text{-F})_2)_2][BF_4]$, **1a**, was isolated. Yield: 0.040 g (74%). The dihydrogen complexes **2a–5a** were prepared by a similar procedure. The synthetic details are given in the Supporting Information. The NMR spectral data of these complexes have been collected in Table 2. The mass spectral data of the complexes are as follows. **1a**: $m/z = 1189$ [$M^+ - (H_2 + BF_4^-)$], 1153 [$M^+ - (H_2 + Cl^- + BF_4^-)$]. **2a**: $m/z = 1046$ [$M^+ - (H_2 + BF_4^-)$]. **3a**: $m/z = 1122$ [$M^+ - (H_2 + Cl^- + BF_4^-)$]. **4a**: $m/z = 1122$ [$M^+ - (H_2 + Cl^- + BF_4^-)$].

Preparation of $trans\text{-}[Ru(\eta^2\text{-HD})(Cl)(PP)_2][BF_4]$ ($PP = (ArCH_2)_2PCH_2CH_2P(CH_2Ar)_2$, $Ar = p\text{-FC}_6H_4$ -, **1a-d, C_6H_5 -, **2a-d**, $m\text{-CH}_3C_6H_4$ -, **3a-d**, $p\text{-CH}_3C_6H_4$ -, **4a-d**, $p\text{-}^iPrC_6H_4$ -, **5a-d**).** Deuterium gas was purged through a solution of $trans\text{-}[Ru(\eta^2\text{-H}_2)(Cl)((p\text{-FC}_6H_4CH_2)_2PC_2H_4P(CH_2C_6H_4p\text{-F})_2)_2][BF_4]$ (0.020 g, 0.014 mmol) in 0.6 mL of CD_2Cl_2 for 30 min with the sample

- (10) (a) Albeniz et al. proposed that isotope scrambling between a dihydrogen complex and D_2 gas takes place due to a combination of the lability and acidity of the dihydrogen ligand: Albeniz, A. C.; Heinekey, D. M.; Crabtree, R. H. *Inorg. Chem.* **1991**, *30*, 3632–3635. (b) Bautista, M. T.; Earl, K. A.; Maltby, P. A.; Morris, R. H.; Schweitzer, C. T.; Sella, A. J. *Am. Chem. Soc.* **1988**, *110*, 7031–7036. (c) Chinn, M. S.; Heinekey, D. M.; Payne, N. G.; Sofield, C. D. *Organometallics* **1989**, *8*, 1824–1826. (d) Earl, K. A.; Jia, G.; Maltby, P. A.; Morris, R. H. *J. Am. Chem. Soc.* **1991**, *113*, 3027–3039. (e) Chin, B.; Lough, A. J.; Morris, R. H.; Schweitzer, C. T.; D'Agostino, C. *Inorg. Chem.* **1994**, *33*, 6278–6288.

Table 2. 1H and $^31P\{^1H\}$ NMR Spectral Data (δ) of $trans\text{-}[Ru(\eta^2\text{-H}_2)(Cl)((ArCH_2)_2PCH_2CH_2P(CH_2Ar)_2)_2][BF_4]$ ($Ar = p\text{-FC}_6H_4$ -, **1a**), C_6H_5 -, **2a**), $m\text{-CH}_3C_6H_4$ -, **3a**), $p\text{-CH}_3C_6H_4$ -, **4a**), $p\text{-}^iPrC_6H_4$ -, **5a**) Complexes in CD_2Cl_2

compd no./Ar	$\delta(Ru-\eta^2\text{-H}_2)$	$\delta(CH_2CH_2)$	1H		$J(H,H)$, Hz	$\delta(Ar-R)$	$\delta(Ar)$	$^31P\{^1H\}$	
			$\delta(CH_2Ar)$	$\delta(PP)$				$\delta(PP)$	$\delta(PP)$
1a / $p\text{-FC}_6H_4$ - ^a	-13.82 (br s, 2H)	0.86 (br s, 4H), 1.02 (br s, 4H)	2.66–4.11 (br m, 16H)		14.7, 16.0, 14.7, 16.0	6.71–7.85 (br m, 32H)		52.3 (s)	
2a / C_6H_5 -	-13.78 (br s, 2H)	0.88 (br s, 4H), 1.34 (br s, 4H)	2.82 (d, 4H), 2.96 (d, 4H), 3.23 (d, 4H), 4.86 (d, 4H)		14.6, 13.6, 14.7	6.82–7.45 (br m, 40H)		54.3 (s)	
3a / $m\text{-CH}_3C_6H_4$ -	-13.79 (br s, 2H)	0.84 (br s, 4H), 1.14 (br s, 4H)	2.82 (br s, 4H), 3.11 (d, 4H), 3.43 (d, 4H), 4.07 (d, 4H)		16.6, 13.6, 14.2	6.68–7.70 (br m, 32H)		53.8 (s)	
4a / $p\text{-CH}_3C_6H_4$ -	-13.88 (br s, 2H)	0.78 (br s, 4H), 1.27 (br s, 4H)	2.79 (br s, 8H), 3.13 (br s, 8H)			6.60–7.96 (br m, 32H)		55.2 (s)	
5a / $p\text{-}^iPrC_6H_4$ -	-13.79 (br s, 2H)	0.81 (br s, 8H)	2.30 (d, 4H), 3.07 (d, 4H), 4.05 (d, 4H) ^b			6.69–7.39 (br m, 32H)		53.1 (s)	

^a ^{19}F NMR: -150.7 (s, ArF), -151.7 (s, ArF), 144.3 (br s, BF_4). ^b The fourth doublet signal overlaps with the multiplet of the CH moiety of the ⁱPr group. ^c $J(H,H) = 7.8$ Hz.

Table 3. H, D Coupling Constant and the d_{HH} (Å) Data for *trans*-[Ru(η^2 -HD)(Cl)(PP)₂][BF₄] (PP = (ArCH₂)₂PCH₂CH₂P(CH₂Ar)₂, Ar = *p*-FC₆H₄– (1a-d₁), C₆H₅– (2a-d₁), *m*-CH₃C₆H₄– (3a-d₁), *p*-CH₃C₆H₄– (4a-d₁), *p*-^{*i*}PrC₆H₄– (5a-d₁) and [Ru(η^2 -HD)(PP)₂][OTf]₂ (PP = (ArCH₂)₂PCH₂CH₂P(CH₂Ar)₂, Ar = *m*-CH₃C₆H₄– (6a-d₁), *p*-CH₃C₆H₄– (7a-d₁))

compd no./Ar	$\delta(\text{Ru}-\eta^2\text{-HD})$	$J(\text{H},\text{D}), \text{Hz}$	$J(\text{HD},\text{P}_{\text{cis}}), \text{Hz}$	$d_{\text{HH}}, \text{Å}$
1a-d ₁ / <i>p</i> -FC ₆ H ₄ – ^a	–13.88 (1:1:1 t qnt)	26.4 ± 0.3	6.8 ± 0.2	0.975 ± 0.005
2a-d ₁ /C ₆ H ₅ –	–13.82 (1:1:1 t qnt)	25.4 ± 0.1	6.8 ± 0.1	0.992 ± 0.001
3a-d ₁ / <i>m</i> -CH ₃ C ₆ H ₄ –	–13.81 (1:1:1 t) ^a	24.9 ± 0.1		1.001 ± 0.001
4a-d ₁ / <i>p</i> -CH ₃ C ₆ H ₄ –	–13.95 (1:1:1 t qnt)	24.4 ± 0.2	6.8 ± 0.1	1.016 ± 0.003
5a-d ₁ / <i>p</i> - ^{<i>i</i>} PrC ₆ H ₄ –	–13.82 (1:1:1 t) ^a	23.4 ± 0.3		1.035 ± 0.005
6a-d ₁ / <i>m</i> -CH ₃ C ₆ H ₄ –	–18.05 (1:1:1 t qnt)	22.4 ± 0.1	8.8 ± 0.3	1.041 ± 0.001
7a-d ₁ / <i>p</i> -CH ₃ C ₆ H ₄ –	–18.07 (1:1:1 t qnt)	22.0 ± 0.2	7.8 ± 0.2	1.052 ± 0.003

^a Obtained from ¹H{³¹P} NMR spectra.

tube dipped in an ice–salt mixture. The sample tube was then set on a rotary shaker for one-half an hour for deuterium incorporation. The HD isotopomer^{10a} *trans*-[Ru(η^2 -HD)(Cl)((*p*-FC₆H₄CH₂)₂PC₂H₄P(CH₂C₆H₄-F)₂)]₂[BF₄], 1a-d₁, was observed by NMR spectroscopy by nullifying the residual signal due to the η^2 -H₂ species using an inversion recovery pulse.^{10b–e} Complexes 2a-d₁, 3a-d₁, 4a-d₁, and 5a-d₁ were prepared similarly. The HD coupling constant data are summarized in Table 3.

Preparation of [Ru(H)(PP)₂][OTf] (PP = (ArCH₂)₂PCH₂CH₂P(CH₂Ar)₂, Ar = *m*-CH₃C₆H₄–, 6, *p*-CH₃C₆H₄–, 7). To a CD₂-Cl₂ solution (0.6 mL) of *trans*-[Ru(H)(Cl)((*m*-H₃C–C₆H₄CH₂)₂PC₂H₄P(CH₂C₆H₄-*m*-CH₃)₂)]₂, 3 (0.020 g, 0.017 mmol), in a 5 mm NMR tube, cooled to 273 K, was added MeOTf (3.9 μ L, 0.031 mmol), and it was shaken for 15 min. The colorless solution turned yellow, resulting in formation of [Ru(H)((*m*-H₃C–C₆H₄CH₂)₂PC₂H₄P(CH₂C₆H₄-*m*-CH₃)₂)]₂[OTf], 6. Compound 7 was prepared similarly. Both of these complexes were found to be quite unstable, and attempts to isolate them resulted in the decomposed material; therefore, they were characterized by NMR spectroscopy only in solution. The NMR spectral data for these complexes are summarized in Table 4.

Preparation of [Ru(η^2 -H₂)(PP)₂][OTf]₂ (PP = (ArCH₂)₂PCH₂CH₂P(CH₂Ar)₂, Ar = *m*-CH₃C₆H₄–, 6a, *p*-CH₃C₆H₄–, 7a). The NMR tubes containing solutions of the five-coordinate complexes, 6 and 7 prepared as described above, were cooled to 195 K, and then 2 equiv of HOTf (2.8 μ L, 0.03 mmol) was added. The yellow-colored solutions turned reddish-yellow. The dihydrogen complexes [Ru(η^2 -H₂)(PP)₂][OTf]₂ (PP = (ArCH₂)₂PCH₂CH₂P(CH₂Ar)₂, Ar = *m*-CH₃C₆H₄–, 6a, *p*-CH₃C₆H₄–, 7a) were characterized in solution by NMR spectroscopy. The NMR spectral features of these complexes are summarized in Table 5.

Preparation of [Ru(η^2 -HD)(PP)₂][OTf]₂ (PP = (ArCH₂)₂PCH₂CH₂P(CH₂Ar)₂, Ar = *m*-CH₃C₆H₄–, 6a-d₁, *p*-CH₃C₆H₄–, 7a-d₁). To the NMR tubes containing the five-coordinate complexes, 6 and 7 at 195 K, prepared as described above, was added 2 equiv of DOTf (2.8 μ L, 0.03 mmol), and it was shaken for 10 min. The HD isotopomers formed [Ru(η^2 -HD)(PP)₂][OTf]₂ (PP = (ArCH₂)₂PCH₂CH₂P(CH₂Ar)₂, Ar = *m*-CH₃C₆H₄–, 6a-d₁, *p*-CH₃C₆H₄–, 7a-d₁) were characterized using NMR spectroscopy. The residual signal due to the η^2 -H₂ moiety in these derivatives were nullified using an inversion recovery pulse.^{10b–e} The HD coupling constant data are summarized in Table 3.

X-ray Structure Determination of *trans*-[Ru(η^2 -H₂)(Cl)-((C₆H₅CH₂)₂PCH₂CH₂P(CH₂C₆H₅)₂)]₂[BF₄], 2a. A suitable crystal was mounted in a glass capillary. The unit cell parameters and intensity data were collected at 293 K on a Bruker SMART APEX CCD diffractometer equipped with a fine-focus Mo K α X-ray source. The SMART software package was used for data acquisi-

Table 4. ¹H, ³¹P{¹H}, and ¹⁹F NMR Spectral Data (δ) of [Ru(H)(PP)₂][OTf] (PP = (ArCH₂)₂PCH₂CH₂P(CH₂Ar)₂, Ar = *m*-CH₃C₆H₄– (6), *p*-CH₃C₆H₄– (7)) Complexes in CD₂Cl₂

compd no./Ar	$\delta(\text{Ru}-\text{H})$	$J(\text{H},\text{P}_{\text{cis}}), \text{Hz}$	¹ H		$\delta(\text{Ar}-\text{R})$	$\delta(\text{Ar})$	³¹ P		¹⁹ F	
			$\delta(\text{CH}_2\text{CH}_2)$	$\delta(\text{CH}_2\text{Ar})$			$\delta(\text{PP})$	$\delta(\text{OTf})$		
6/ <i>m</i> -CH ₃ C ₆ H ₄ –	–25.03 (qnt, 1H)	20.5	0.76–0.87 (br s, 8H)	2.76–3.52 (m, 16H)	2.30 (br m, 24H)	6.54–7.89 (br m, 32H)	59.1 (s)	–79.9 (s)		
7/ <i>p</i> -CH ₃ C ₆ H ₄ –	–24.94 (qnt, 1H)	19.5	0.69–0.85 (br s, 8H)	2.78–3.95 (m, 16H)	2.33 (br m, 24H)	6.23 (d, 8H), ^a 6.72–7.73 (br m, 24H)	59.0 (s)	–79.8 (s)		

^a $J(\text{H},\text{H}) = 6.8 \text{ Hz}$.

Table 5. ^1H , $^{31}\text{P}\{^1\text{H}\}$, and ^{19}F NMR Spectral Data (δ) of $[\text{Ru}(\eta^2\text{-H}_2)(\text{PP})_2][\text{OTf}]_2$ (PP = $(\text{ArCH}_2)_2\text{PCH}_2\text{CH}_2\text{P}(\text{CH}_2\text{Ar})_2$, Ar = $m\text{-CH}_3\text{C}_6\text{H}_4\text{-}$ (**6a**), $p\text{-CH}_3\text{C}_6\text{H}_4\text{-}$ (**7a**)) Complexes in CD_2Cl_2

compd no./Ar	$\delta(\text{Ru}-\eta^2\text{-H}_2)$	$\delta(\text{CH}_2\text{CH}_2)$	^1H			^{31}P	^{19}F
			$\delta(\text{CH}_2\text{Ar})$	$\delta(\text{Ar}-\text{R})$	$\delta(\text{Ar})$	$\delta(\text{PP})$	$\delta(\text{OTf})$
6a / $m\text{-CH}_3\text{C}_6\text{H}_4\text{-}$	-18.06 (br s, 2H)	0.86-1.22 (br s, 8H)	2.65-4.09 (m, 16H)	2.31 (br m, 24H)	6.51-7.94 (br m, 32H)	52.9 (s)	-80.2 (s)
7a / $p\text{-CH}_3\text{C}_6\text{H}_4\text{-}$	-18.09 (br s, 2H)	0.64-1.28 (br s, 8H)	2.70-4.04 (m, 16H)	2.28 (br m, 24H)	6.59-7.85 (br m, 32H)	54.7 (s)	-80.1 (s)

Table 6. Crystallographic Data for $\text{trans-}[\text{Ru}(\eta^2\text{-H}_2)(\text{Cl})((\text{C}_6\text{H}_5\text{CH}_2)_2\text{PCH}_2\text{CH}_2\text{P}(\text{CH}_2\text{C}_6\text{H}_5)_2)][\text{BF}_4]$, **2a**

formula	$\text{C}_{61}\text{H}_{68}\text{BCl}_3\text{F}_4\text{P}_4\text{Ru}$
fw	1219.26
cryst syst	triclinic
space group	$\bar{P}1$
a , Å	11.935(3)
b , Å	14.451(4)
c , Å	17.166(5)
α , deg	77.478(4)
β , deg	87.307(4)
γ , deg	79.995(4)
V , Å ³	2846.2(13)
Z	2
D_{calcd} , g/cm ³	1.423
T , K	293(2)
λ , Å	0.71073
μ , mm ⁻¹	0.581
R^a	0.0400
R_w^a	0.1033

^a $R = \Sigma(|F_o| - |F_c|)/\Sigma|F_o|$; $R_w = [\Sigma w(|F_o| - |F_c|)^2/\Sigma w|F_o|^2]^{1/2}$ (based on reflections with $I > 2\sigma(I)$).

Table 7. Selected Bond Lengths (Å) and Angles (deg) for $\text{trans-}[\text{Ru}(\eta^2\text{-H}_2)(\text{Cl})((\text{C}_6\text{H}_5\text{CH}_2)_2\text{PCH}_2\text{CH}_2\text{P}(\text{CH}_2\text{C}_6\text{H}_5)_2)][\text{BF}_4]$ **2a**

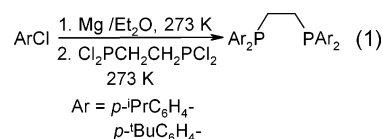
H(100)-H(101)	1.08(5)	Ru(1)-P(3)	2.3755(9)
Ru(1)-P(1)	2.3776(8)	Ru(1)-P(4)	2.3571(8)
Ru(1)-P(2)	2.3514(9)	Ru(1)-Cl(1)	2.4453(8)
P(1)-Ru(1)-P(2)	83.37(3)	P(3)-Ru(1)-P(4)	82.64(3)
P(1)-Ru(1)-P(3)	173.71(3)	P(1)-Ru(1)-Cl(1)	88.08(3)
P(1)-Ru(1)-P(4)	95.39(3)	P(2)-Ru(1)-Cl(1)	86.33(3)
P(2)-Ru(1)-P(3)	98.72(3)	P(3)-Ru(1)-Cl(1)	86.14(3)
P(2)-Ru(1)-P(4)	178.21(3)	P(4)-Ru(1)-Cl(1)	94.93(3)

tion, and the SAINT software package was used for data reduction.¹¹ Absorption corrections were made using the SADABS program¹² and empirical method.¹³ The structure was solved and refined using the SHELX programs.¹⁴ The ruthenium atom position was observed by the Patterson method, and the non-hydrogen atoms were located by successive difference Fourier maps and refined anisotropically. The hydrogen atoms attached to ruthenium were located from the difference Fourier map and refined isotropically. All other hydrogen atoms were generated in idealized positions and refined in a riding model. The crystallographic data are summarized in Table 6, and the pertinent bond lengths and angles are listed in Table 7.

Results and Discussion

Ligand Synthesis. A set of bis-1,2(dibenzylphosphino)ethane ligands of the type $(\text{ArCH}_2)_2\text{PCH}_2\text{CH}_2\text{P}(\text{CH}_2\text{Ar})_2$ (Ar = $p\text{-FC}_6\text{H}_4\text{-}$, $\text{C}_6\text{H}_5\text{-}$, $m\text{-CH}_3\text{C}_6\text{H}_4\text{-}$, $p\text{-CH}_3\text{C}_6\text{H}_4\text{-}$, $p\text{-}^i\text{PrC}_6\text{H}_4\text{-}$, $p\text{-}^t\text{BuC}_6\text{H}_4\text{-}$) were prepared following the procedure reported by Kubas and co-workers.³ These ligands were obtained by treatment of $\text{Cl}_2\text{PCH}_2\text{CH}_2\text{PCL}_2$ with the ap-

propriate Grignard reagent in Et_2O at 273 K in fairly good yields (eq 1). The magnesium metal required for preparation of the Grignard reagents must be activated mechanically by vigorously agitating under Ar for 48 h.⁸ The diphosphine ligands are highly moisture sensitive in solution but stable in the solid state in air for a few hours without getting oxidized. The $(p\text{-}^t\text{Bu}-\text{C}_6\text{H}_4\text{CH}_2)_2\text{PCH}_2\text{CH}_2\text{P}(\text{CH}_2\text{C}_6\text{H}_4\text{-}p\text{-}^t\text{Bu})_2$ ligand was found to be extremely unstable in solution, getting rapidly oxidized even in the presence of trace quantities of oxygen. The oxidized ligand shows a singlet at δ 20.1 in the $^{31}\text{P}\{^1\text{H}\}$ NMR spectrum.



The Hammett constants (σ) of the substituents on the benzyl moiety of the phosphine phosphorus systematically vary along this series from the substituent: $p\text{-F}$ (0.06), H (0), $m\text{-CH}_3$ (-0.07), $p\text{-CH}_3$ (-0.17), $p\text{-}^i\text{Pr}$ (not available), $p\text{-}^t\text{Bu}$ (-0.20), reflecting their electron-donor abilities in that order.¹⁵ There is, however, no perfect correlation between the Hammett constants and the $^{31}\text{P}\{^1\text{H}\}$ NMR chemical shifts of these ligands.

Synthesis of $\text{trans-}[\text{Ru}(\text{H})\text{Cl}((\text{ArCH}_2)_2\text{PCH}_2\text{CH}_2\text{P}(\text{CH}_2\text{Ar})_2)]$ (Ar = $p\text{-FC}_6\text{H}_4\text{-}$, **1**, $\text{C}_6\text{H}_5\text{-}$, **2**, $m\text{-CH}_3\text{C}_6\text{H}_4\text{-}$, **3**, $p\text{-CH}_3\text{C}_6\text{H}_4\text{-}$, **4**, $p\text{-}^i\text{PrC}_6\text{H}_4\text{-}$, **5**). The ruthenium hydride chloride complexes (**1-5**) were prepared by reacting $[\text{Ru}(\text{H})\text{Cl}(\text{PPh}_3)_3]$ with the appropriate diphosphine ligand adopting the procedure reported by Manuel et al. for certain analogous hydride derivatives (eq 2).¹⁶ These new hydride complexes, isolated as yellow or reddish-yellow solids, are stable in air for short periods of time. The $^{31}\text{P}\{^1\text{H}\}$ NMR spectra consist of only one resonance for all the phosphorus atoms, indicating the planar disposition of the chelating phosphines and the hydride and the chloride ligands, in trans conformation. Attempts to prepare the $\text{trans-}[\text{Ru}(\text{H})\text{Cl}((p\text{-}^t\text{Bu}-\text{C}_6\text{H}_4\text{CH}_2)_2\text{PCH}_2\text{CH}_2\text{P}(\text{CH}_2\text{C}_6\text{H}_4\text{-}p\text{-}^t\text{Bu})_2)]$ complex were unsuccessful; we always ended up getting the oxidized ligand together with some unreacted starting ruthenium complex.

The ^1H NMR chemical shifts for the hydride hydrogen fall in the range from -19.63 to -19.98; the chemical shifts do not correlate with the Hammett constants, although the electron-donor ability increases from the $p\text{-F}$ to the $p\text{-}^i\text{Pr}$ substituent in this series of complexes. The ^1H NMR spectra consist of a quintet resonance for the hydride hydrogen due to coupling with the four *cis*-phosphorus atoms with $J(\text{H},$

(11) SMART and SAINT, version 6.22a; Bruker AXS: Madison, WI, 1999.

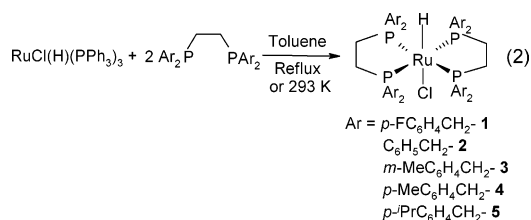
(12) Sheldrick, G. M. SADABS, version 2; Multiscan Absorption Correction program; University of Göttingen: Göttingen, Germany, 2001.

(13) Blessing, R. H. Acta Crystallogr., Sect. A **1995**, 51, 33-38.

(14) Sheldrick, G. M. SHELXL-97 Program for the solution of Crystal Structures; University of Göttingen: Göttingen, Germany, 1997.

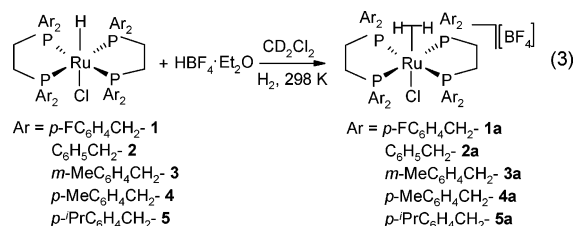
(15) Blackburn, E. V.; Tanner, D. D. J. Am. Chem. Soc. **1980**, 102, 692-697.

(16) Manuel, J.-T.; Carmen, M. P.; Valerga, P. Inorg. Chem. **1994**, 33, 3515-3520.



$\nu_{\text{cis}} = 19.5\text{--}20.0$ Hz and the two methylene hydrogens of the benzyl groups are diastereotopic showing up as four doublets with geminal couplings ranging from 12.6 to 17.6 Hz. However, in the case of the $p\text{-}^i\text{Pr}$ complex, three doublets are well resolved whereas the fourth one overlaps with other signals. Similar spectral characteristics were noted earlier for a series of molybdenum complexes bearing benzylphosphine-based coligands.³ The $^{31}\text{P}\{^1\text{H}\}$ NMR chemical shifts experience upfield shifts, albeit small, with increasing basicities of the chelating phosphine ligand.

Preparation and Properties of $\text{trans}[\text{Ru}(\eta^2\text{-H}_2)(\text{Cl})(\text{ArCH}_2)_2\text{PCH}_2\text{CH}_2\text{P}(\text{CH}_2\text{Ar})_2][\text{BF}_4]$ ($\text{Ar} = p\text{-FC}_6\text{H}_4\text{-}$, **1a, $\text{C}_6\text{H}_5\text{-}$, **2a**, $m\text{-CH}_3\text{C}_6\text{H}_4\text{-}$, **3a**, $p\text{-CH}_3\text{C}_6\text{H}_4\text{-}$, **4a**, $p\text{-}^i\text{PrC}_6\text{H}_4\text{-}$, **5a**).** Protonation of the hydride complexes **1–5** using $\text{HBF}_4 \cdot \text{OEt}_2$ resulted in the dihydrogen complexes **1a–5a** (eq 3). These dihydrogen complexes were found to be quite stable, and therefore, isolation in the solid state was possible in the cases of **1a–4a**, whereas **5a** was characterized in solution only by NMR spectroscopy. The products were obtained in fairly good yields. Crystals suitable for X-ray crystallographic study were obtained in the case of **2a**.



The ^1H NMR spectra of the dihydrogen complexes consist of a broad singlet for the bound H_2 ligand in the range from $\delta -13.78$ to -13.88 . As in the precursor hydrides, the benzylic hydrogens in the dihydrogen complexes are diastereotopic, showing up either as four doublets or as broad multiplets. The $^{31}\text{P}\{^1\text{H}\}$ NMR spectra consist of only one resonance for all four phosphorus atoms, indicating that the four P atoms of the chelating phosphines are equivalent and that the trans disposition of the Cl and the dihydrogen ligand is retained upon protonation. The $^{31}\text{P}\{^1\text{H}\}$ NMR chemical shifts are upfield shifted with respect to the starting hydride derivatives.

The intact nature of the H–H bond in these complexes was established from the variable-temperature ^1H spin-lattice relaxation time (T_1 , ms; 400 MHz) measurements. The T_1 data have been deposited in the Supporting Information. A plot of T_1 (ms) versus temperature (K) shows the typical

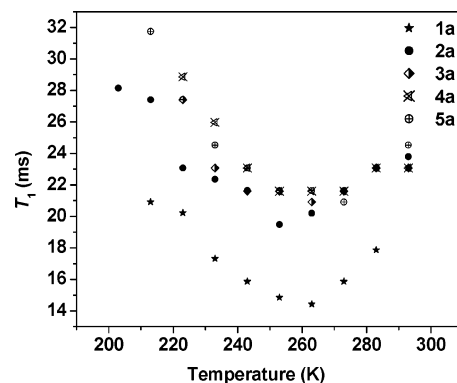


Figure 1. Plot of T_1 (400 MHz) versus temperature for complexes **1a–5a**.

parabolic behavior as shown in Figure 1.¹⁷ The T_1 minima together with the H–H distances (d_{HH} (slow and fast), Å) calculated from T_1 (min) have been tabulated in the Supporting Information.¹⁸ T_1 (min) ranges from 14 to 22 ms. More definitive evidence for the intact nature of the H–H bond in these derivatives was obtained from the $J(\text{H},\text{D})$ couplings for the HD isotopomers. The HD isotopomers **1a-d1**, **2a-d1**, **3a-d1**, **4a-d1**, and **5a-d1** were prepared by treating the $\eta^2\text{-H}_2$ complexes with $\text{D}_2(\text{g})$ for long periods of time at 273 K. Due to the overlapping of signals of the $\eta^2\text{-H}_2$ and $\eta^2\text{-HD}$ species, the ^1H NMR spectral signal appeared as a broad singlet with a shoulder upfield to the broad signal. Nullification of the $\eta^2\text{-H}_2$ signal in the ^1H NMR spectrum by the inversion recovery pulse sequence using the relationship $T_1 = \tau_{\text{null}}/\ln 2$ and the known T_1 value of the dihydrogen complex at room temperature^{10b–e} gave the 1:1:1 triplet which is expected for the HD isotopomer. Each of the triplet signals was further split into quintets due to HD– P_{cis} couplings. As a representative example, the HD and HD– P_{cis} couplings in the case of **4a-d1** are shown in Figure 2.

The H–H distances (d_{HH} , Å) in complexes **1a–5a** were calculated from the inverse relationship between the $J(\text{H},\text{D})$ and the d_{HH} ¹⁹ and are listed in Table 3. d_{HH} varies from 0.97 Å to 1.03 Å with a systematic increment, albeit small from **1a** to **5a**. The increase in the H–H distances along this series of dihydrogen complexes is a reflection of the electron-donor ability of the diposphine ligand (Hammett constants: $p\text{-F}$ (0.06), H (0), $m\text{-CH}_3$ (–0.07), $p\text{-CH}_3$ (–0.17), $p\text{-}^i\text{Pr}$ (not available)), increasing along this order: $\text{Ar} = p\text{-FC}_6\text{H}_4\text{-} < \text{C}_6\text{H}_5\text{-} < m\text{-CH}_3\text{C}_6\text{H}_4\text{-} < p\text{-CH}_3\text{C}_6\text{H}_4\text{-} < p\text{-}^i\text{PrC}_6\text{H}_4\text{-}$. A plot of the $J(\text{H},\text{D})$ versus the appropriate σ values of these ligands is shown in Figure 3. It is interesting to note that Axenrod et al. observed a linear correlation between the ^{15}N –H coupling constants and the appropriate Hammett σ constants

- (17) (a) Luo, X.-L.; Crabtree, R. H. *Inorg. Chem.* **1990**, *29*, 2788–2791. (b) Luo, X.-L.; Howard, J. A. K.; Crabtree, R. H. *Magn. Reson. Chem.* **1991**, *29*, S89–S93. (c) Desrosiers, P. J.; Cai, L.; Lin, Z.; Richards, R.; Halpern, J. *J. Am. Chem. Soc.* **1991**, *113*, 4173–4184.
- (18) Morris, R. H.; Wittebort, R. *J. Magn. Reson. Chem.* **1997**, *35*, 243–250.
- (19) (a) Heinekey, D. M.; Luther, T. A. *Inorg. Chem.* **1996**, *35*, 4396–4399. (b) Maltby, P. A.; Schlaf, M.; Steinbeck, M.; Lough, A. J.; Morris, R. H.; Klooster, W. T.; Koetzle, T. F.; Srivastava, R. C. *J. Am. Chem. Soc.* **1996**, *118*, 5396–5407.

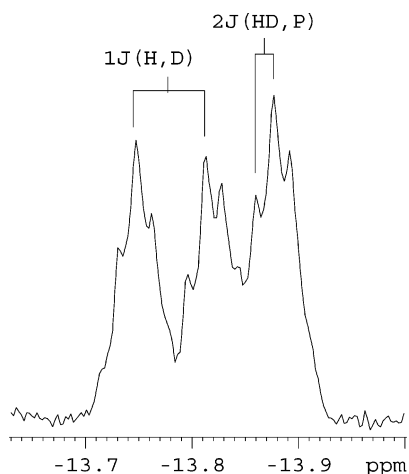


Figure 2. ^1H NMR spectrum (hydride region) of $\text{trans-}[\text{Ru}(\eta^2\text{-HD})(\text{Cl})\text{-}((\text{C}_6\text{H}_5\text{-CH}_2)_2\text{PCH}_2\text{CH}_2\text{P}(\text{CH}_2\text{C}_6\text{H}_5)_2)_2][\text{BF}_4]$ **2a-d₁** (400 MHz, 293 K) in CD_2Cl_2 .

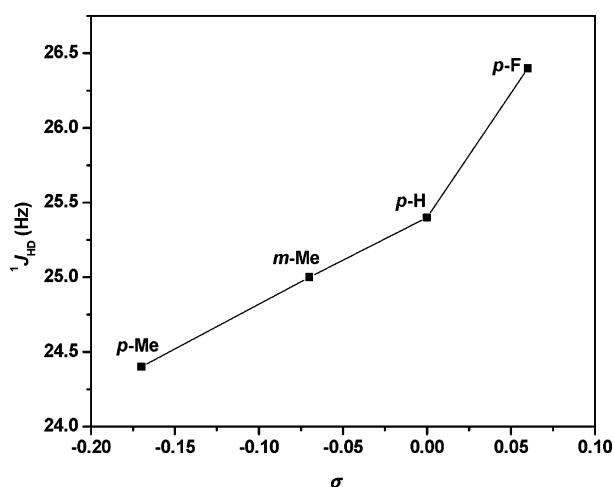


Figure 3. Plot of $J(\text{H},\text{D})$ of **1a-d₁**–**4a-d₁** versus Hammett constants (σ) of the substituent on the benzyl ligand.

in a series of substituted aniline- ^{15}N derivatives.²⁰ It was found that the magnitude of the coupling constants decreased with an increase in the donor property of the substituent. Similarly, Hess and co-workers²¹ found a linear relationship between the methyl ^{13}C – ^1H coupling constants and Hammett σ constants of the substituents for a series of substituted toluenes, anisoles, and other similar aromatic compounds. In addition, Cobley and Pringle established a correlation between the Pt–P bond strength and the Hammett substituent constants via examination of the $^1J(\text{Pt},\text{P})$ and σ values.²²

The complexes **3a–5a** can be categorized as *elongated* dihydrogen complexes since the d_{HH} in these derivatives is ≥ 1.0 Å. The elongated dihydrogen complexes represent the arrested intermediate states of the oxidative addition of H_2 to a metal center. Some of the complexes that are pertinent to the current work are (a) $\text{trans-}[\text{Ru}(\eta^2\text{-H}_2)\text{Cl}(\text{Ph}_2\text{PCH}_2\text{CH}_2\text{-PPh}_2)]^+$ ($J(\text{H},\text{D}) = 25.9$ Hz, $d_{\text{HH}} = 0.99$ Å; $\sigma_{\text{p}} = 0.009$, $\sigma_{\text{m}} = 0.218$), (b) $\text{trans-}[\text{Ru}(\eta^2\text{-H}_2)\text{Cl}(\text{Et}_2\text{PCH}_2\text{CH}_2\text{PEt}_2)]^+$ ($J(\text{H},\text{D})$

$= 25.2$ Hz, $d_{\text{HH}} = 1.00$ Å), and (c) $\text{trans-}[\text{Ru}(\eta^2\text{-H}_2)\text{Cl}(\text{Cy}_2\text{-PCH}_2\text{CH}_2\text{PCy}_2)]^+$ ($J(\text{H},\text{D}) = 16.0$ Hz, $d_{\text{HH}} = 1.15$ Å).^{19b,23} This data suggests that there is a correlation between the donor abilities of the substituents on the phosphine phosphorus and the $J(\text{H},\text{D})$ and in turn the d_{HH} . In addition to an attempt by Kubas and co-workers to study the reaction coordinate for H_2 cleavage by the electronic control of the dihydrogen versus the dihydride coordination in certain molybdenum complexes,³ there has been only one other systematic study,²⁴ although to a lesser extent, of an investigation of the type presented in the current work. The d_{HH} shows a great deal of variation in the dihydrogen complexes reported to date, from 0.82 Å all the way up to 1.5 Å along the reaction coordinate for the activation of H_2 .^{1,2,17c,18,19b,25,26} The study of the binding and elongation of H_2 and the arrested intermediate states on its way to oxidative addition to a metal center is extremely important because it serves as a prototype for the other σ -bond activation processes, e.g., C–H bond and Si–H bond. Although elongation of the H–H bond length in the complexes reported herein is not very appreciable, it is instructive to note that it is possible to design systems such that the H–H bond could be substantially elongated and at the same time in an incremental order as if mapping out the reaction coordinate for the oxidative addition of H_2 to a metal center. Efforts toward this goal are in progress in our laboratories.

X-ray Crystal Structure of $\text{trans-}[\text{Ru}(\eta^2\text{-H}_2)\text{Cl}\text{-}((\text{C}_6\text{H}_5\text{CH}_2)_2\text{PCH}_2\text{CH}_2\text{P}(\text{CH}_2\text{C}_6\text{H}_5)_2)_2][\text{BF}_4]$, **2a.** The ORTEP diagram of the cation is shown in Figure 4. Pertinent bond lengths and angles are summarized in Table 7. The structure consists of an octahedron with the four phosphine phosphorus atoms lying in a square plane and the chloride approximately perpendicular to this plane. The sixth coordination site is occupied by the dihydrogen ligand which is bound in an η^2 -fashion. The hydrogen atoms of the H_2 ligand were located

(20) Axenrod, T.; Pregosin, P. S.; Wieder, M. J.; Milne, G. W. A. *J. Am. Chem. Soc.* **1969**, *91*, 3681–3682.

(21) Yoder, C. H.; Tuck, R. H.; Hess, R. E. *J. Am. Chem. Soc.* **1969**, *91*, 539–543.

(22) Cobley, C. J.; Pringle, P. G. *Inorg. Chim. Acta* **1997**, *265*, 107–115.

(23) The Hammett constants (σ_{p} and σ_{m}) have been obtained from studies of compound $\text{XC}_6\text{H}_4\text{COOH}$: (a) Hansch, C.; Leo, A.; Taft, W. R. *Chem. Rev.* **1991**, *91*, 165–195. (b) Jaffe, H. H. *Chem. Rev.* **1953**, *53*, 191–261. (c) Hammett constant data are not available for the cyclohexyl substituent.

(24) Cappellani, E. P.; Drouin, S. D.; Jia, G.; Maltby, P. A.; Morris, R. H.; Schweitzer, C. T. *J. Am. Chem. Soc.* **1994**, *116*, 3375–3388.

(25) (a) Crabtree, R. H. *Acc. Chem. Res.* **1990**, *23*, 95–101. (b) Jessop, P. G.; Morris, R. H. *Coord. Chem. Rev.* **1992**, *121*, 155–284. (c) Heinekey, D. M.; Oldham, W. J., Jr. *Chem. Rev.* **1993**, *93*, 155–284. (d) Morris, R. H. *Can. J. Chem.* **1996**, *74*, 1907–1915. (e) Kuhlman, R. *Coord. Chem. Rev.* **1997**, *167*, 205–232. (f) Sabo-Etienne, S.; Chaudret, B. *Coord. Chem. Rev.* **1998**, *178–180*, 381–407. (g) Esteruelas, M. A.; Oro, L. A. *Chem. Rev.* **1998**, *98*, 577–588. (h) Jia, G.; Lau, C.-P. *Coord. Chem. Rev.* **1999**, *192*, 83–108. (i) Esteruelas, M. A.; Oro, L. A. *Adv. Organomet. Chem.* **2001**, *47*, 1–59.

(26) (a) Matthews, S. L.; Heinekey, D. M. *J. Am. Chem. Soc.* **2006**, *128*, 2615–2620. (b) Yousufuddin, M.; Wen, T. B.; Mason, S. A.; McIntyre, G. J.; Jia, G.; Bau, R. *Angew. Chem., Int. Ed.* **2005**, *44*, 7227–7230. (c) Grellier, M.; Vendier, L.; Chaudret, B.; Albinati, A.; Rizzato, S.; Mason, S.; Sabo-Etienne, S. *J. Am. Chem. Soc.* **2005**, *127*, 17592–17593. (d) Nanishankar, H. V.; Dutta, S.; Nethaji, M.; Jagirdar, B. R. *Inorg. Chem.* **2005**, *44*, 6203–6210. (e) Ingleson, M. J.; Brayshaw, S. K.; Mahon, M. F.; Ruggiero, G. D.; Weller, A. S. *Inorg. Chem.* **2005**, *44*, 3162–3171. (f) Pons, V.; Heinekey, D. M. *J. Am. Chem. Soc.* **2003**, *125*, 8428–8429. (g) Heinekey, D. M.; Law, J. K.; Schultz, S. M. *J. Am. Chem. Soc.* **2001**, *123*, 12728–12729. (h) Fang, X.; Huhmann-Vincent, J.; Scott, B. L.; Kubas, G. J. *J. Organomet. Chem.* **2000**, *609*, 95–103.

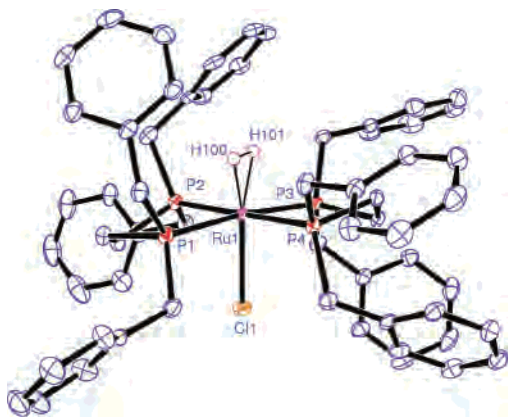
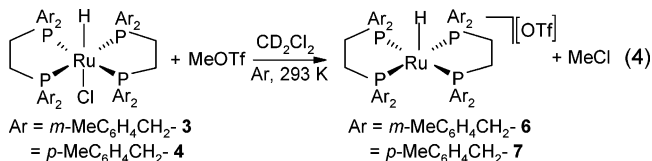


Figure 4. ORTEP view of *trans*-[Ru(η^2 -H₂)(Cl)((C₆H₅CH₂)₂PCH₂CH₂P(CH₂C₆H₅)₂)](BF₄), **2a**, at the 50% probability level.

from the successive difference Fourier maps. H(100)–H(101) was found to be 1.08(5) Å, which can be categorized as an *elongated* dihydrogen ligand. This distance is slightly longer (taking into account the standard deviations) than that obtained from $J(\text{H},\text{D})$ couplings (see above). The two Ru–H bond distances (Ru(1)–H(100) and Ru(1)–H(101)) are, respectively, 1.63(3) and 1.59(3) Å. The four phosphorus atoms and ruthenium atom are in a plane. The Ru–P distances are in the range from 2.3514(9) to 2.3776(8) Å, and the average of these distances is 2.3654 Å. The bite angles P(1)–Ru(1)–P(2) and P(3)–Ru(1)–P(4) are 83.37(3)° and 82.64(3)°, respectively. The Ru(1)–Cl(1) bond length is 2.4453(8) Å which is longer by 0.038 Å in comparison to the dppe analog *trans*-[Ru(η^2 -H₂)Cl(dppe)₂][PF₆] reported by Morris et al.^{10e} This is a reflection of the greater donor ability of the chelating phosphine in **2a** compared to that of dppe (Ph₂PCH₂CH₂PPh₂) in Morris' complex. In the family of dihydrogen complexes with the [Ru(PP)₂] backbone, **2a** is only the fifth complex to be crystallographically characterized.²⁷ The dihydrogen hydrogens in the *trans*-[Ru(η^2 -H₂)Cl(dppe)₂][PF₆] derivative were not located. d_{HH} obtained from X-ray crystallography in the case of *trans*-[Ru(η^2 -H₂)H(dppe)₂][BPh₄] is 0.83(8) Å.²⁸ Our attempts to obtain single crystals suitable for neutron diffraction studies were unsuccessful.

Preparation and Properties of [Ru(η^2 -H₂)(PP)₂][OTf]₂ (PP = (ArCH₂)₂PCH₂CH₂P(CH₂Ar)₂, Ar = *m*-CH₃C₆H₄–, **6a, *p*-CH₃C₆H₄–, **7a**).** We recently reported the synthesis and protonation studies of a five-coordinate, 16-electron complex stabilized by agostic interaction, [Ru(H)((C₆H₅CH₂)₂PCH₂CH₂P(CH₂C₆H₅)₂)]₂[OTf].⁵ This compound was obtained from the corresponding six-coordinate hydride chloride complex by reaction with MeOTf via elimination of MeCl. Similarly, reaction of *trans*-[Ru(H)Cl((ArCH₂)₂PCH₂CH₂P(CH₂Ar)₂)] (Ar = *m*-CH₃C₆H₄–, **3**, *p*-CH₃C₆H₄–, **4**) with MeOTf resulted in the five-coordinate, 16-electron complexes [Ru(H)(PP)₂][OTf] (PP = (ArCH₂)₂PCH₂CH₂P(CH₂Ar)₂),

Ar)₂, Ar = *m*-CH₃C₆H₄–, **6**, *p*-CH₃C₆H₄–, **7**) via MeCl elimination (eq 4).

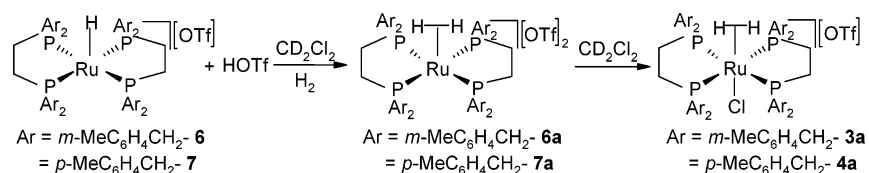


The ¹H NMR spectra of these species show a quintet for the hydride hydrogen that is upfield shifted in comparison to the precursor hydrides at δ –25.03 and –24.94, respectively, for **6** and **7**. The ³¹P{¹H} NMR spectra of **6** and **7** exhibit a single resonance at δ 59.1 and 59.0, respectively. The appearance of a distinct doublet at δ 6.23 ($J(\text{H},\text{H}) = 6.8$ Hz) which is upfield shifted from the remaining phenyl hydrogens (δ 6.72–7.73) could be assigned to the ortho hydrogens of the *p*-methylbenzyl moiety in the case of complex **7** interacting with the metal in an *agostic* fashion in the sixth coordination site. Attempts to isolate **7** resulted in intractable species as ascertained by NMR spectroscopy, which can be attributed to the weak agostic interaction. This is in contrast to the case of [Ru(H)((C₆H₅CH₂)₂PCH₂CH₂P(CH₂C₆H₅)₂)]₂[OTf] which is isolable in the solid state.⁵ On the other hand, we found no evidence of agostic interaction in **6**. It is interesting to note that the sixth coordination site on the metal in **6** is vacant, and attempts to isolate this species in the solid state resulted in extensive decomposition products. The sterically crowded substituted benzyl ligands in complexes **6** and **7** lead to the lack of and weak agostic interaction, respectively; this is reflected in their instabilities. For Ar = *p*-FC₆H₄, the negative inductive effect of the fluorine makes the ortho-H of *p*-FC₆H₄CH₂– less electron donating compared to the others; therefore, in this case, we noted no reaction between MeOTf and *trans*-[Ru(H)Cl((*p*-FC₆H₄CH₂)₂PCH₂CH₂P(CH₂-*p*-FC₆H₄)₂)]₂. Kubas et al. earlier found in a series of molybdenum complexes of the type [Mo(CO)((ArCH₂)₂PCH₂CH₂P(CH₂Ar)₂)]₂ that agostic interaction is favored only for Ar = C₆H₅– and *m*-CH₃C₆H₄–, which has been attributed to the favorable sterics, whereas other aryl groups gave intractable products.³ Complexes **6** and **7** are stable for up to 10–12 h at room temperature in solution after which time they pick up a chloride from the solvent resulting in recovery of the hydride chloride derivatives **3** and **4**, respectively. In order to establish the existence of a vacant site or the agostic interaction with certainty in **6** and **7**, respectively, we treated these derivatives with CH₃CN. In both cases, the nitrile products *trans*-[Ru(H)(CH₃CN)(PP)₂][OTf] (PP = (ArCH₂)₂PCH₂CH₂P(CH₂Ar)₂, Ar = *m*-CH₃C₆H₄–, **8**, *p*-CH₃C₆H₄–, **9**) were obtained almost instantaneously (eq 5). In addition, the ¹⁹F NMR spectra of complexes **6** and **7** show only one signal (δ –79.0) suggesting that there is only one type of triflate, namely, counterion, rather than a counterion and a bound triflate. Variable-temperature ¹H NMR spectroscopy of **7** resulted in the broadening of the doublet signal at δ 6.23 (agostic hydrogen) at low temperature, eventually becoming a broad singlet at 243 K. The signal was also slightly upfield shifted.

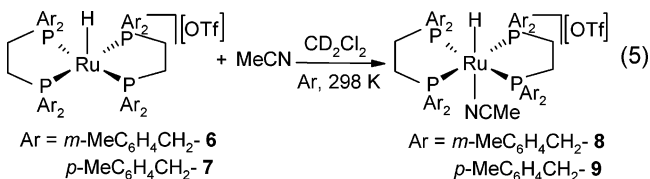
(27) (a) Jimenez-Tenorio, M.; Puerta, M. C.; Valerga, P. *J. Chem. Soc., Chem. Commun.* **1993**, 1750–1751. (b) Schlaf, M.; Lough, A. J.; Morris, R. H. *Organometallics* **1997**, *16*, 1253–1259.

(28) Albinati, A.; Klooster, W. J.; Koetzle, T. F.; Fortin, J. B.; Ricci, J. S.; Eckert, J.; Fong, T. P.; Lough, A. J.; Morris, R. H.; Golombek, A. P. *Inorg. Chim. Acta* **1997**, *259*, 351–357.

Scheme 1



Further cooling to 223 K resulted only in the broad signal merging with the baseline; we could not discern any fluxional process.



Protonation of the five-coordinate complexes **6** and **7** using HOTf in CD_2Cl_2 gave the dicationic dihydrogen complexes $[\text{Ru}(\eta^2\text{-H}_2)((\text{ArCH}_2)_2\text{PCH}_2\text{CH}_2\text{P}(\text{CH}_2\text{Ar})_2)][\text{OTf}]_2$ ($\text{Ar} = m\text{-MeC}_6\text{H}_4\text{-}$, **6a**, $p\text{-MeC}_6\text{H}_4\text{-}$, **7a**). The bound H_2 ligand in these complexes appears as a broad singlet that is downfield shifted with respect to the precursor hydrides. $^{31}\text{P}\{^1\text{H}\}$ NMR spectroscopy showed only a single resonance for all four phosphine P atoms, evidencing that the structural motif is not perturbed upon protonation. The agostic interaction noted in complex **7** disappeared upon protonation. No evidence for the binding of either the triflate counterion or the solvent in the sixth coordination site of the metal in freshly prepared solutions of **6a** and **7a** was found. The ^{19}F NMR spectra of **7** and **7a** showed only the resonance of the triflate counterion that remained invariant even at low temperatures (see Supporting Information). In addition, protonation of **7** in 1,2-dichloroethane (external lock, acetone- d_6) did not show significant differences in the spectral features of **7a** compared to that performed in CD_2Cl_2 (see Supporting Information). This further rules out the binding of the solvent in the vacant site around the metal center. However, with time, **6a** and **7a** pick up a chloride from the solvent CD_2Cl_2 to generate the six-coordinate complexes **3a** and **4a** (Scheme 1).

The intact nature of the H–H bond in complexes **6a** and **7a** was established from the variable-temperature ^1H spin–lattice relaxation time measurements (Table S3, Supporting Information) and the $J(\text{H},\text{D})$ couplings of the corresponding HD isotopomers **6a-d₁** and **7a-d₁**. The HD and HD–P_{cis} couplings ($J(\text{H},\text{D}) = 22.0 \pm 0.2$) in the case of complex **7a-d₁** are shown in Figure 5.

d_{HH} for these complexes were found to be 1.04 and 1.05 Å, respectively. It is interesting to note that **6a** and **7a** are unprecedented examples of five-coordinate, 16-electron, dicationic elongated dihydrogen complexes of ruthenium. Related examples of 16-electron, elongated dihydrogen complexes of ruthenium with agostic interactions of the type $[\text{Ru}(\text{H})(\text{X})(\eta^2\text{-H}_2)(\text{PCy}_3)_2]$ ($\text{X} = \text{Cl}, \text{Br}, \text{SR}$) have been reported by Chaudret and co-workers previously.²⁹

Electronic Influence of Coligands on the H–H Bond Elongation. The well-established two-component binding involves H_2 to $\text{M}(\text{d}) \sigma$ donation and $\text{M}(\text{d}\pi)$ to $\text{H}_2(\sigma^*)$ back-

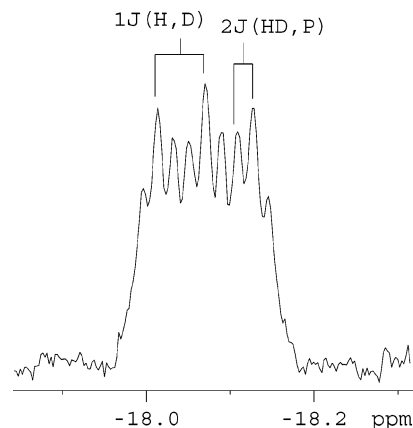


Figure 5. ^1H NMR spectrum of the hydride region of $[\text{Ru}(\eta^2\text{-HD})((p\text{-MeC}_6\text{H}_4\text{-CH}_2)_2\text{PCH}_2\text{CH}_2\text{P}(\text{CH}_2\text{C}_6\text{H}_4\text{-}p\text{-Me})_2)][\text{OTf}]_2$, **7a-d₁**.

donation. The $\text{M}(\text{d}\pi)$ to $\text{H}_2(\sigma^*)$ back-donation can weaken the H–H bond, but the degree of back-donation controls H–H bond cleavage due to the population of the σ^* orbital of the bound H_2 .³⁰ Kubas et al. established the binding of the dihydrogen ligand (intact H–H bond) in $[\text{Mo}(\eta^2\text{-H}_2)(\text{CO})(\text{dppe})_2]$ ($\text{dppe} = \text{Ph}_2\text{PCH}_2\text{CH}_2\text{PPh}_2$), whereas H_2 undergoes oxidative addition in molybdenum complexes of the type $[\text{Mo}(\eta^2\text{-H}_2)(\text{CO})(\text{R}_2\text{PCH}_2\text{CH}_2\text{PR}_2)_2]$ ($\text{R} = \text{Et}, \text{Bu}^i$).³¹ Although the cone angles of PPh_3 and P^iBu_3 are very similar, 145° and 143° , respectively,³² the dihydrogen versus dihydride binding is dictated by the electronics rather than sterics (cone angles in this case).³³ The extent of back-donation is controlled by the diphosphine basicity, which in turn directs the H–H bond elongation; no steric influence in the form of cone angles of the phosphines was found to play a role.

- (29) (a) Toner, A.; Matthes, J.; Gründemann, S.; Limbach, H.-H.; Chaudret, B.; Clot, E.; Sabo-Etienne, S. *Proc. Natl. Acad. Sci.* **2007**, *104*, 6945–6950. (b) Toner, A.; Gründemann, S.; Clot, E.; Limbach, H.-H.; Donnadiou, B.; Sabo-Etienne, S.; Chaudret, B. *J. Am. Chem. Soc.* **2000**, *122*, 6777–6778.
- (30) (a) Saillard, J.-Y.; Hoffmann, R. *J. Am. Chem. Soc.* **1984**, *106*, 2006–2026. (b) Low, J. J.; Goddard, W. A. *J. Am. Chem. Soc.* **1984**, *106*, 8321–8322. (c) Nakatsuji, H.; Hada, M. *J. Am. Chem. Soc.* **1985**, *107*, 8264–8266. (d) Jean, Y.; Eisenstein, O.; Volatron, F.; Maoche, B.; Sefta, F. *J. Am. Chem. Soc.* **1986**, *108*, 6587–6592. (e) Hay, P. J. *J. Am. Chem. Soc.* **1987**, *109*, 705–710. (f) Burdett, J. K.; Phillips, J. R.; Pourian, M. R.; Poliakov, M.; Tumer, I. J.; Upmacis, R. *Inorg. Chem.* **1987**, *26*, 3054–3063.
- (31) (a) Kubas, G. J.; Ryan, R. R.; Wroblewski, D. A. *J. Am. Chem. Soc.* **1986**, *108*, 1339–1341. (b) Kubas, G. J.; Ryan, R. R.; Unkefer, C. J. *J. Am. Chem. Soc.* **1987**, *109*, 8113–8115. (c) Kubas, G. J.; Burns, C. J.; Eckert, J.; Johnson, S. W.; Larson, A. C.; Vergamini, P. J.; Unkefer, C. J.; Khalsa, G. R. K.; Jackson, S. A.; Eisenstein, O. *J. Am. Chem. Soc.* **1993**, *115*, 569–581.
- (32) (a) Tolman, C. A. *Chem. Rev.* **1977**, *77*, 313–348. (b) Tolman, C. A.; Seidel, W. C.; Gosser, L. W. *J. Am. Chem. Soc.* **1974**, *96*, 53–60.
- (33) (a) Bautista, M.; Earl, K. A.; Morris, R. H.; Sella, A. *J. Am. Chem. Soc.* **1987**, *109*, 3780–3782. (b) Bautista, M. T.; Earl, K. A.; Morris, R. H. *Inorg. Chem.* **1988**, *27*, 1124–1125. (c) Bautista, M. T.; Cappellani, E. P.; Drouin, S. D.; Morris, R. H.; Schweitzer, C. T.; Sella, A.; Zubkowski, J. *J. Am. Chem. Soc.* **1991**, *113*, 4876–4887.

As a consequence of the flexibility of the benzyl groups, the effective cone angle of $\text{P}(\text{CH}_2\text{C}_6\text{H}_5)_3$ was found to be 142° , which is very similar to that of P^iBu_3 .³⁴ Therefore, in the $^i\text{Bu}_2\text{PCH}_2\text{CH}_2\text{P}^i\text{Bu}_2$ ligand and its benzyl counterpart, despite having similar steric properties, weaker basicity of the benzyl diphosphine ligand is expected to stabilize the $\eta^2\text{-H}_2$ binding mode. The reaction coordinate for the oxidative addition of H_2 to the molybdenum center in the molybdenum–diphosphine complexes reported by Kubas et al. is rather flat until it is quite close to cleavage of the H–H bond. This indicates that there will be very little change in the H–H bond distance until bond cleavage is imminent. On the other hand, the series of cationic complexes reported by Morris et al. $[\text{MH}(\eta^2\text{-H}_2)(\text{R}_2\text{PCH}_2\text{CH}_2\text{PR}_2)]^+$ ($\text{M} = \text{Fe}, \text{Ru}$) do not show H–H bond cleavage as the substituent is varied in a similar fashion.³³ This means that H–H is farther away from the point of cleavage on the reaction coordinate. The positive charge on the molecule could stabilize $\eta^2\text{-H}_2$ binding over dihydride formation via reduced $\text{Ru}(\text{d}\pi)\text{-H}_2$ (σ^*) back-donation. Recent work of Heinekey and co-workers on a family of complexes of the type $[\text{Ru}(\text{Cp})/(\text{Cp}^*)(\eta^2\text{-H}_2)(\text{PP})]^+$ showed that the phosphine ligand variation had a profound effect on the temperature dependence of the $J(\text{H},\text{D})$.³⁵ They found that the variations in the electronic properties of the chelating phosphines resulted in subtle changes in the $\text{Ru}\text{-H}_2$ binding, suggesting that such ligand variation will have a significant effect on the vibrational potential of the bound H_2 . In the series of complexes presented in this report, **1a–5a**, the H–H distance increases from **1a** to **5a** reflecting the increasing basicity of the diphosphine or a decrease in the Hammett constants of the benzyl substituent from *p*-fluorobenzyl to *p*-iso-propylbenzyl. The incremental increase, although small, follows an expected trend.

(34) Barron, A. R. *J. Chem. Soc., Dalton Trans.* **1988**, 3047–3050.

(35) Law, J. K.; Mellows, H.; Heinekey, D. M. *J. Am. Chem. Soc.* **2002**, *124*, 1024–1030.

Conclusions

The protonation reactions of the hydride complexes of the type $\text{trans-}[\text{Ru}(\text{H})\text{Cl}((\text{ArCH}_2)_2\text{PCH}_2\text{CH}_2\text{P}(\text{CH}_2\text{Ar})_2)_2]$ ($\text{Ar} = p\text{-FC}_6\text{H}_4\text{-}$, **1**, $\text{C}_6\text{H}_5\text{-}$, **2**, $m\text{-CH}_3\text{C}_6\text{H}_4\text{-}$, **3**, $p\text{-CH}_3\text{C}_6\text{H}_4\text{-}$, **4**, $p\text{-}^i\text{PrC}_6\text{H}_4\text{-}$, **5**) with $\text{HBF}_4\cdot\text{OEt}_2$ result in the corresponding dihydrogen complexes $\text{trans-}[\text{Ru}(\eta^2\text{-H}_2)(\text{Cl})((\text{ArCH}_2)_2\text{PCH}_2\text{CH}_2\text{P}(\text{CH}_2\text{Ar})_2)_2][\text{BF}_4]$. The H–H bond distances, d_{HH} , vary in small increments from 0.97 to 1.03 Å, correlating with the donor properties of the substituents (Hammett constants) on the benzyl moiety of the chelating phosphine ligands. Thus, it should be possible to construct dihydrogen complexes along the reaction coordinate for the oxidative addition of H_2 to a metal center by suitably altering the coligands in a systematic manner such that the donor ability of the coligands increases in small increments.

Reaction of $\text{trans-}[\text{Ru}(\text{H})\text{Cl}((\text{ArCH}_2)_2\text{PCH}_2\text{CH}_2\text{P}(\text{CH}_2\text{Ar})_2)_2]$ ($\text{Ar} = m\text{-CH}_3\text{C}_6\text{H}_4\text{-}$, **3**, $p\text{-CH}_3\text{C}_6\text{H}_4\text{-}$, **4**) with MeOTf results in five-coordinate species of the type $[\text{Ru}(\text{H})((\text{ArCH}_2)_2\text{PCH}_2\text{CH}_2\text{P}(\text{CH}_2\text{Ar})_2)_2][\text{OTf}]$ via elimination of MeCl . Protonation of these complexes results in the corresponding five-coordinate elongated dihydrogen complexes $[\text{Ru}(\eta^2\text{-H}_2)((\text{ArCH}_2)_2\text{PCH}_2\text{CH}_2\text{P}(\text{CH}_2\text{Ar})_2)_2][\text{OTf}]_2$ which are unprecedented.

Acknowledgment. We thank the Department of Science & Technology, India, with gratitude for financial support. We also thank the DST, India, for funding the procurement of the X-ray diffractometer and a 400 MHz NMR spectrometer under the “FIST” grant. We are grateful to the Department of Organic Chemistry, I.I.Sc., for providing access to the mass spectral facility.

Supporting Information Available: X-ray crystallographic data for $\text{trans-}[\text{Ru}(\eta^2\text{-H}_2)(\text{Cl})((\text{C}_6\text{H}_5\text{CH}_2)_2\text{PCH}_2\text{CH}_2\text{P}(\text{CH}_2\text{C}_6\text{H}_5)_2)_2][\text{BF}_4]$, **2a**, in CIF format, details of the synthesis of the complexes, VT ^1H spin–lattice relaxation time (T_1 , ms; 400 MHz) data for the dihydrogen complexes, VT NMR spectral stack plots, and the mass spectral data for the complexes. This material is available free of charge via the Internet at <http://pubs.acs.org>.

IC7016769